Middle Pleistocene climate and hydrological environment at the Boxgrove hominin site (West Sussex, UK) from ostracod records

Jonathan A. Holmes[1], Environmental Change Research Centre, Department of Geography, University College London, London, WC1E 6BT, UK

Tim Atkinson, Bloomsbury Environmental Isotope Facility, Department of Chemistry, University College London, London, WC1H 0AJ, UK

D. P. Fiona Darbyshire, NERC Isotope Geosciences Laboratory, Kingsley Dunham Centre, Keyworth, Nottingham, NG12 5GG, UK

David J. Horne, Department of Geography, Queen Mary University of London, London E1 4NS, UK, and Department of Zoology, The Natural History Museum, Cromwell Road, London, SW7 5BD, UK

José Joordens, Department of Sedimentology and Marine Geology, Vrije Universiteit Amsterdam, De Boelelaan 1085,1081 HV Amsterdam, the Netherlands

Mark B. Roberts, Institute of Archaeology, University College London, London, WC1H 0PY, UK

Katharine J. Sinka, School of Environmental Sciences, University of East Anglia, Norwich NR4 7TJ, UK

John E. Whittaker, Department of Palaeontology, The Natural History Museum, Cromwell Road, London, SW7 5BD, UK

[1]. Corresponding author; telephone +44 207 679 0559 email j.holmes@ucl.ac.uk

Abstract

The sediments of the Slindon Formation at the junction of the Chalk South Downs and the West Sussex Coastal Plain, as revealed and studied at Boxgrove, contain evidence for early Middle Pleistocene environments in southern England around half a million years ago. The archaeological importance of the deposits is attested to by the recovery of stone and organic tools, butchered fauna and fossil hominin remains. We combine palaeoecological and geochemical analyses of ostracods from the coastal plain deposits to reconstruct the climate and environment at one period of the hominin occupation. The stratigraphy of our study area is indicative of a terrestrial environment surrounding a small lake or pond. Ostracod assemblages from the pond sediments indicate that they were shallow but permanent, and fed by groundwater and springwater. However, the species alone cannot confirm that these ponds were completely fresh. Application of Mutual Climatic Range (MCR) techniques shows that summer temperatures were similar to present-day values and winter temperatures were probably colder, whereas mean annual air temperature was similar to present or perhaps slightly cooler. Trace-element and strontium-isotope analyses of ostracods from the pond sediments support the conclusion that they were fed largely by fresh groundwater derived from the chalk, although there may have been a minor seawater input. The carbon isotope ratios of the ostracod shells are also consistent with a groundwater source, although they also indicate that the dissolved inorganic carbon most likely did not reach equilibrium with atmospheric carbon dioxide,

indicating that the ponds had short residence time. The combination of palaeotemperature estimates with oxygen-isotope values from ostracod shells allowed us to reconstruct the oxygen-isotope ratio of the pondwater, which was close to the value of early Middle Pleistocene precipitation at this site. Values were similar to present day, suggesting that there may have been a change in seasonality or precipitation source, since the mean air temperatures might have been lower.

1. Introduction

An understanding of hominin evolution and distribution requires knowledge of the physical and biotic environment in which each species lived. Although large-scale reconstructions using, for example, marine sediments provide a valuable environmental context for hominin evolution, they must be complemented by smaller-scale, site-specific environmental investigations from localities close to where the hominin remains have been found. Here, we use a novel combination of ostracod-based palaeoecological and geochemical data to reconstruct environmental conditions at Boxgrove, an important early Palaeolithic site in southern England.

Ostracods are microscopic aquatic crustaceans. The occurrence of different ostracod species is determined by habitat type and by ecological factors such as water temperature and composition (Smith and Horne, 2002). They secrete shells of low-Mg calcite that are often well preserved in Quaternary sediments. Ostracod faunal assemblages have been used for palaeoecological reconstructions of past environment. Moreover their shells have been used in numerous geochemical and isotopic studies (Holmes and Chivas, 2002). However, quantitative palaeoecological reconstructions have not hitherto been combined with geochemical analyses of material from the same site in the approach that we adopt here.

Eartham Quarry (50˚51’52”N, 0˚39;06”W), in the Parish of Boxgrove, is located on the northern edge of the West Sussex Coastal Plain in southern England (Fig. 1) (Roberts et al., 1994). An interglacial sea-level event towards the end of the early Middle Pleistocene ‘Cromerian Complex’ (likely Marine Isotope Stage 13) cut a cliff into the Cretaceous Upper Chalk and Palaeogene Reading Beds and London Clay, and led to the formation of the Westbourne – Arundel 40 metre raised beach. During the early Middle Pleistocene, the southerly extension of the Weald – Artois Anticlinorum provided a substantial connection with the European mainland, to the east and west of the present Strait of Dover. The early Middle Pleistocene topography on the West Sussex Coastal Plain was also substantially different to that of the present day. A further range of chalk downland was present to the south, comprising the hills of the Portsdown and Littlehampton Anticlines (Fig. 1). The MIS 13 marine transgression entered through the gap between the distal ends of the anticlinal limbs and led to the formation of a semi-enclosed marine bay (Barnes 1980), backed at the northern edge by the 40 metre OD Westbourne to Arundel Raised Beach (Fig. 1). A massive tibia and two incisors assigned to *Homo* cf. *heidelbergensis* have been found in association with Lower Palaeolithic stone tools at Eartham Quarry (Roberts et al., 1994; Pitts and Roberts, 1996). The remains were found in Units 4u (incisors) and 5ac (tibia) of the marine/freshwater/terrestrial sequence found at area Q1/B (Table 1). Apart from the hominin remains, human presence at the site, indicated by stone tools and butchered bones, is found within all the sedimentary units from which the ostracod samples were taken. On the basis of foraminiferal and ostracod assemblages, these sediments are shown to have been deposited in a regressive sea followed by a fully nonmarine setting (Whittaker, 1999). The nonmarine sediments represent a localised landscape of ponds and slow-flowing

streams that existed at this part of the abandoned coastal plain, the so-called 'pond facies' in which the hominin remains were found. These freshwater sediments were surrounded by an extensive, coeval, terrestrial landscape, the deposits of which are rich in stone tools and other palaeoenvironmental remains. The ‘pond facies’ contain abundant ostracods, *Chara* oospores, fish remains, slug plates, mammals, birds, herpetofauna, and earthworm granules and eggs. We used the rich, well-preserved ostracod faunas from the pond facies to reconstruct the climatic and hydrological environment of the coastal plain at the time of hominin occupation. We combined ostracod faunal assemblage analyses with estimates of air temperature using a mutual ostracod temperature range (MOTR) method (Horne, 2007), supported by previous mutual climate range (MCR) reconstructions from herpetofaunas (Sinka, 1993), with trace-element (Sr/Ca and Mg/Ca) and isotope ($^{18}O/^{16}O$, $^{13}C/^{12}C$, $^{87}Sr/^{86}Sr$) analyses to address the following questions. (1) What was the source of water feeding the coastal plain ponds? (2) Was the water purely fresh or saline? (3) What was the mean annual and seasonal temperature regime of the coastal plain?

Because there is no longer an extant waterbody present at or near the coastal plain, we analysed water chemistry and ostracods from small, groundwater-fed ponds at Greywell (Hampshire, UK; Fig.1), which lies ~50 km NNW of Boxgrove, for which we have detailed monthly records of ostracod assemblages and water composition over an annual cycle (Keatings, 1999; Keatings et al., 2002). The ponds at Greywell lie in a similar setting to the coastal plain ponds, albeit without any possibility of marine influence, and thus provide a useful modern analogue.

2. Stratigraphy and palaeoenvironment

The standard conformable stratigraphical sequence at Boxgrove consists of the nearshore marine sands of the Slindon Sand Member (Unit 3 of the standard sequence) overlain by intertidal laminated muds of the Slindon Silt Member, which were laid down in a semi-enclosed marine bay, and finally by terrestrial deposits (Table 1).

At Quarry 1/B, however, this stratigraphical sequence is significantly altered. Here, Unit 3 has been truncated and subjected to pedogenesis and ripening. Locally, a large, northwest-to-southeast-trending channel and several smaller channels were cut into its surface. The main channel, which has a maximum depth of 0.8 m, is infilled with a coarse gravel deposit at the base, containing flint beach pebbles, worked flint and bone fragments and an arenaceous, fine component with some chalky clay deposition with fine to massive bedding (Figs. 2 and 3, Table 1).

The channel deposits are completely overlain by Unit 4u, the basal unit of the pond sequence, and its associated minor sub-unit 4.4u(s). Elsewhere, Unit 4u only partially covers the Unit 3 surface, although whether this distribution mirrors its original deposition or is the result of subsequent erosion is unclear. This unit is a massive silt with rare traces of bedding, although in places a sandier facies Unit 4u(s), indicating higher energy deposition, has been noted. Unit 4u is overlain by Unit 4, the thickest and most extensive of the pond deposits, which consists of a relatively homogenous, dense, massive silt. This unit has been heavily disturbed by pore water release deformation structures from dewatering, most especially towards its surface. The upper pond deposits consist of Unit 4d1, a highly calcareous white silt of variable thickness that contains intraformational calcrete nodules. Unit 4d1 is overlain by the highly mixed sediments of Unit 5ac, a poorly sorted coarse silt, with

subrounded chalk clasts and sand-size quartz grains. Bedding is occasionally present along with organic laminae similar to, but thinner than, Unit 5a. The sediments of Unit 5ac are a mix of redeposited pond sediments combined with upslope colluvial deposits. Unit 5ac is succeeded by a return to highly calcareous spring deposition of Units 4d2 and 4d3, which are in turn overlain by the marker horizon and upper bed of the Slindon Silt Member, Unit 5a. This bed, between 10 and 15mm thick has recently been mapped over a distance of 15km, between Adsdean and Slindon, by Roberts and Pope (in press). Unit 5a comprises many microlaminations of detrital organic material and was deposited in an alder/fen carr environment that developed on top of the Slindon Silts. The colluvial sedimentation that overlies Unit 5a sees a reversion to the standard stratigraphic sequence seen elsewhere at Boxgrove.

The pond sediments described here were deposited under fully interglacial conditions, as demonstrated by the taxonomic composition of the mammalian and herpetofaunas (Roberts and Parfitt, 1999). The excavated freshwater sediments lie some 50 to 80 metres south of the relict cliff line, with an east – west dimension of about 100 metres and a south – north distribution that has been proven, on the basis of facies distribution, to be at least 40 metres, but which probably extended to the cliff line itself. The locale, which would have been rich in terrestrial and aquatic vegetation, was utilised by many elements of the Boxgrove fauna, including hominins. The remains of butchered rhinoceroses, deer and other animals point to it being a place of food procurement and processing as well as a water source. The whole of the depositional sequence at Q1/B from the basal channel deposits up to the surface of Unit 4d3 was time equivalent and thus a chronostratigraphic correlative

of Unit 4c, the soil bed that developed on the surface of the Slindon Silts after marine regression (Table 1) (Roberts and Parfitt 1999).

Evidence of hominin presence at Boxgrove is found within all the major sedimentary units; from the body of the marine Slindon Sand (Unit 3) and the littoral deposits of the raised beach; up through the regressional marine sands silts; the freshwater deposits at Q1/B; and into the overlying terrestrial sediments. The archaeological signatures of these hominins are best preserved in the marine Slindon Silts of Unit 4b; the terrestrial soil horizon of Unit 4c; and at Q1/B, in the temporal correlatives of the soil horizon – the freshwater pond facies Units 3c, 3/4, 4u, 4, 4d1, 5ac, 4d2 and 4d3 (Table 1). Hominins were therefore operating at the site under widely differing climatic and environmental regimes, ranging from fully temperate littoral through to periglacial tundra. Throughout the time of occupation and exploitation the archaeological record is dominated by evidence for the collection of flint from the actively eroding chalk cliff and the butchery of predominantly large mammals across the temporally changing landscapes in front of the cliff. The site at Q1/B differs from the rest of the excavated locales at Boxgrove in that an extended vertical sediment stack is present, due to the formation of a large spring-fed freshwater pond or waterhole that was cut into the intertidal muds of the Slindon Silt Member. Archaeological remains in the form of lithic and organic artefacts and butchered faunal remains have been recovered from all the freshwater units and suggest that this area was actively used by hominins as both a semi permanent freshwater source and fixed hunting locale in the landscape. The presence of game at the waterhole is attested to by the high level of dung derived mineralised organic material at the base of the waterhole, and the skeletal remains of both butchered and natural death assemblage individuals. The most comprehensive evidence of butchery is found on

the remains of at least five rhinoceroses excavated from the freshwater sediments. The bones of these animals point to accumulation as the result of hunting, as butchery marks indicate first access to the carcasses by hominins and no pathological evidence for natural death in these prime of life adults and juveniles. Other species butchered in the vicinity of the waterhole include giant deer, red deer, horse and bison.

The environment at the waterhole would have changed through time, becoming progressively more heavily vegetated after marine regression. The impact of the freshwater seepage would have become immediately apparent after the sea level fell away and is shown in the sedimentary record by the main and subsidiary channels cut through the Slindon Silt and Sand. The freshwater body then gradually expanded probably by a combination of channel convergence and increased spring flow, to produce the current mapped disposition of the waterhole/pond. The water body then proceed to fill up with reworked marine sediments from the upper part of the sands and to a greater extent the silts, at the surface of the pond increasing amounts calcareous sedimentation are found in Units 4d1, 4d2 and 4d3. Early evidence for the influx of slope material into the water body is found in Unit 5ac, although this input is believed to have occurred under very wet rather than cold conditions. The emplacement of cold stage geliflucted and soliflucted sediments began with Unit 6b and culminated in the burial of the site by mass movement deposits derived from cliff collapse material and the Downland regolith.

3. Materials and analytical methods

We analyzed ostracods from Units 3c, 4u and 4u(s) exposed in Quarry 1/B (Fig. 3). Ostracod assemblage analysis, based on presence and absence of species, was

used to assess the hydrological environment of the coastal plain and the salinity of the ponds. Ostracod identifications were confirmed using descriptions in Meisch (2000) and ecological affinities of individual species were obtained from Robinson (1998), Griffiths and Holmes (2000) and Meisch (2000). Foraminifera tests found in many of the samples were identified using descriptions in Murray (1979). Well-preserved adult or A-1 specimens of three ostracod taxa, namely *Prionocypris zenkeri*, *Candona neglecta* and *Ilyocypris gibba/bradyi* were selected for individual geochemical analysis. These species were chosen because they are relatively abundant in the Slindon Silts freshwater sediments and two of the genera have been the subject of previous geochemical studies (*Ilyocypris*: Holmes et al., 1992; *Candona*: von Grafenstein et al., 1999). Any differences in geochemical vital effects generally occur at the genus level, so our inability to distinguish confidently between the two species of *Ilyocypris* is unlikely to have had any influence on any of the geochemical values. Specimens lacking signs of dissolution or diagenetic alteration were picked from the dried, coarse (>250 μm) sediment fraction and cleaned using a '0000' paintbrush and high-purity deionised water.

Clean ostracod valve material was placed into acid-washed 5ml polypropylene tubes and dissolved in 1 ml 0.6M Merck Aristar® HCl for trace-element analyses. The Ca, Mg, and Sr contents of the ostracod valves were determined using a JY-70 Plus® inductively coupled plasma-atomic emission spectrometer (ICP-AES) calibrated using multi-element standards prepared with Spectrosol® standard solutions for ICP. The results were corrected for blank contamination in the solvent acid and for instrumental drift using an external drift monitor. Multiple analyses of an 'in-house' calcite were undertaken to enable comparisons to be made between analyses performed on different occasions and to assess analytical precision. Based on

multiple analyses of this standard, precision was ±0.6% RSD (relative standard deviation) for Ca, ±0.2% RSD for Mg and ±0.4% RSD for Sr.

Samples of between 5 and 7 ostracod shells weighing in total between ~70 and 100 µg destined for stable isotope analysis were brush-cleaned and air dried before loading into Labco glass Exetainer® tubes. Oxygen and carbon isotope analyses were made on CO_2 produced by reaction with phosphoric acid at 45˚C in a ThermoFisher Gasbench II connected to a Delta V mass spectrometer. Results were expressed in standard δ units on the VPDB scale with a mean standard deviation of measurements of 0.12 ‰ and 0.16 ‰ for $\delta^{18}O$ and $\delta^{13}C$, respectively.

Samples composed of between 3 and 5 ostracod or foraminiferal specimens for Sr-isotope analysis were dissolved in dilute (3%) acetic acid. After centrifuging, the solution was evaporated and the residue converted to chloride with 6M HCl. Strontium was separated by standard ion exchange techniques using BioRad® AG-50W resin and loaded on rhenium filaments with a TaF activator following the method of Birck (1986). Water samples from our modern analogue site at Greywell were filtered in the laboratory through Nalgene® filtration units fitted with 0.45 µm nylon membranes. 5 ml aliquots were evaporated and the residue treated with 6M HCl. After chemical separation involving ion exchange procedures strontium was loaded on tantalum filaments prepared with phosphoric acid. Isotope ratio measurements were made on a Finnegan MAT 262® mass spectrometer run in multidynamic mode. The measured ratios were normalised to a value of 0.710248 for the NBS 987 Sr isotope standard. Replicate determinations (n=66) of North Atlantic seawater standard yielded a $^{87}Sr/^{86}Sr$ ratio of 0.709174 ± 0.000023 (2σ).

4. Results and discussion

4.1. Hydrological environment

The samples from the pond facies of Quarry 1/B contain a low diversity assemblage. Species present, in order of decreasing abundance, are *Candona neglecta, Ilyocypris* cf. *bradyi*, *Herpetocypris reptans, Prionocypris zenkeri, I. quinculminata,* and *Potamocypris zschokkei*. The assemblages show minimal systematic stratigraphical or spatial variations within Quarry 1/B, except locally where they additionally include *Cavernocypris subterraneana.* The presence of adults and a range of juvenile moults from all of the units indicates that the ostracod assemblages are *in situ* and have not been subjected to significant post mortem transport (Whatley, 1988). Foraminiferal tests were also found in most samples derived from the parent units 4a and 4b, the marine Slindon Silt, suggesting that they were reworked from the marine sediments. The species present, in order of decreasing abundance, are *Elphidium williamsoni*, *Haynesina germanica*, *Ammonia falsobeccarii* and *Cibicides lobatulus*.

The habitat preferences of the ostracod species (Table 2) indicate that the pond facies overlying the channels were laid down in small, permanent but shallow, ponds cut into and redepositing the marine deposits of the coastal plain, probably fed by springs or groundwater seepage and supporting rich aquatic vegetation. The presence of aquatic vegetation is confirmed by the abundance of charophyte oogonia within the sediments. Although all of the ostracod taxa are essentially freshwater species, those for which information is available can tolerate elevated salinity, up to about 16 ‰ (Table 2), so the possibility that the coastal plain ponds were slightly saline cannot be ruled out on the basis of the ostracod assemblages alone. The foraminfera species found within the pond facies are also highly euryhaline (Murray, 1979). However, although the ostracods are unlikely to have been transported, as

discussed above, the foraminifera may have been reworked from the regressive shallow-marine deposits, from which ostracods are absent. Moreover, unequivocal ostracod indicators of elevated salinity, such as *Cyprideis torosa, Heterocypris salina* and *Candona angulata* (e.g. Meisch, 2000), are absent from the ostracod assemblages. On balance therefore, the faunal evidence does not suggest that the salinity of the ponds was markedly elevated.

4.2. Air-temperature reconstruction

Air temperature reconstructions were made using two similar but distinct mutual range methods that have been developed independently for ostracods (Horne, 2007) and herptiles (Sinka, 1993). Both methods are similar in principle to the MCR technique described for Coleoptera by Atkinson et al. (1986, 1987). They rely on first calibrating the climatic tolerance ranges of individual species within a two-dimensional space defined by climate variables, then establishing the degree of mutual overlap between all species present in a fossil assemblage (Sinka and Atkinson 1999; Horne and Mezquita 2008)

For ostracods, we estimated past mean annual air temperature (MAAT) as well as July and January by applying the Mutual Ostracod Temperature Range (MOTR) method described by Horne (2007). The MAAT ranges of the ostracod species were calculated specifically for this study, using the same GIS and database as Horne & Mezquita (2008). The MOTR method calibrates each species' tolerance range for mean July temperature and mean January temperature. These two variables are treated separately, leading to a box-shaped area being identified as the mutual range on a plot of one against the other (Fig. 4A). Five extant species that could be identified with certainty were utilised in the MOTR air-temperature reconstructions for

Boxgrove, namely *Candona neglecta*, *Cavernocypris subterraneana*, *Herpetocypris reptans*, *Potamocypris zschokkei* and *Prionocypris zenkeri*. Two taxa found in the deposits, *Ilyocypris quinculminata* and *Ilyocypris* cf. *bradyi*, were excluded because of extinction and taxonomic uncertainty, respectively. The MOTR yielded palaeo air temperature ranges of +14 to + 20 ˚C (July) and -4 to +4 ˚C (January) with a mean annual temperature of +5 to 11 ˚C (Fig. 4B). Present-day (1959-2006 means) instrumental values for nearby Eastbourne are +17 ˚C (July), +6 ˚C (January) and +11 ˚C (mean annual temperature). This indicates MIS-13 summer temperatures for Boxgrove similar to present day, while winter and mean annual temperatures may have been similar but could have been significantly colder.

Sinka (1993) applied the Mutual Climatic Range (MCR) method of Atkinson et al. (1986, 1987) to the Pleistocene herpetofaunas reported for British interglacial deposits, including Boxgrove. The MCR method differs from the MOTR in that it used a different climate data base, and also in that species' ranges are determined within a space defined by T_{MAX}, the mean temperature of the warmest calendar month, and T_{RANGE}, the difference between warmest and coldest months. Because T_{MAX} is close to July mean temperature, and $T_{MAX} – T_{RANGE} = T_{MIN}$ is close to January mean temperature, the results from the two methods should be comparable with one another. An important difference, however, is that whereas the MOTR method calibrates species with respect to one variable at a time, the herptile MCR approach considers both climate variables simultaneously. Consequently the mutual climatic range (MCR) area for Boxgrove herptiles is irregular in shape, in contrast to the rectangular area for the ostracod MOTR (Fig.4C).

361 The Boxgrove herpetofauna includes the following six species that were used in the
362 MCR: *Anguis fragilis* (Slow worm), *Rana temporaria* (Common frog), *Rana arvalis*
363 (Moor frog), *Bufo bufo* (Common toad), *Pelobates fuscus (*Common spadefoot toad)
364 and *Triturus vulgaris* (Smooth newt) (Holman, 1999). Since the original herpetofaunal
365 MCR was constructed, additional species have been identified from the freshwater
366 sediments at Boxgrove Q1/B by the late J.A. Holman: these are *Triturus cristatus*
367 (Crested Newt),*Triturus helveticus* (Palmate Newt), *Rana (ridibunda)* sp.
368 (Indeterminate European Water Frogs), *Pelodytes punctatus* (Common Parsley
369 Frog), *Bufo calamita* (Natterjack Toad), *Lacerta vivipara* (Viviparous Lizard), *Natrix*
370 *natrix* (Grass Snake) and *Coronella austriaca* (Smooth Snake). Although these
371 additional species have not been included in the existing herpetofauna MCR, they
372 would be unlikely to alter the reconstructed temperatures significantly.
373
374 The herptile remains from Boxgrove were recovered mainly from Unit 4C (Holman,
375 1999), and therefore lie stratigraphically close to the units from which the ostracods
376 were found. The MCR encompasses a range from 15 to 24 ^{o}C for T_{MAX}, -12 to +4 ^{o}C
377 for T_{MIN}, and 2 to 13 ^{o}C for MAAT. The present climate for Eastbourne lies outside
378 the MCR (Fig. 4), confirming the result from the MOTR method that the Boxgrove
379 climate during MIS-13 may have had similar summer temperatures to present day,
380 but that the seasonal range was greater and winter temperatures could have been
381 significantly colder.
382
383 A further refinement is to combine the MOTR and MCR ranges to produce estimated
384 ranges for summer, winter and mean annual air temperatures that are compatible for
385 both groups of organisms. In Fig. 4C, the ostracod MOTR is superimposed on the

herptile MCR, using the assumed relationships, July mean temperature ≈ T_{MAX}, January mean temperature ≈ T_{MIN} and the exact equation, $T_{RANGE} = T_{MAX} – T_{MIN}$. The combined range for T_{MAX} is 15 to 20 ^{o}C, for T_{MIN} –4 to +4 ^{o}C and for MAAT 5 to 12 ^{o}C. The effect of combining the two groups is to restrict the distributions of MAAT values obtained from each individually, markedly compared with the herptile MCR but only slightly compared with the ostracod MOTR.

4.3. Palaeosalinity

Sr/Ca ratios of un-evaporated waters, such as those of the coastal plain ponds investigated here, reflect water source. The Sr/Ca ratio of ostracod shells provides a proxy for the Sr/Ca of the host water, assuming the species-specific partitioning effects are known. When sea-water is added to freshwater from a single source, the Sr/Ca ratio of the resulting mixture can be described using a simple two-component mixing model. It is possible that the Boxgrove Pond waters were just such two-component mixtures i.e. of chalk-derived shallow groundwater with a small admixture of seawater. Because the Sr content of seawater is much greater than that of many meteoric waters, including very-shallow groundwater derived from chalk, the mixing line is highly non linear with only a small input of seawater (a few percent) required to generate a mixture with a ‘marine’ Sr/Ca ratio. We have no modern measurements of the Sr/Ca ratio of shallow groundwater from the Boxgrove area. However, the site from Greywell provides a useful modern analogue for the meteoric end member of the Boxgrove Pond waters (Keatings, 1999). Here, a series of shallow ponds is fed by shallow groundwater passing through Upper Chalk of similar age (Campanian to Turonian) and facies to Boxgrove, and these have a Sr/Ca_{water} ratio of 0.0012 ± 0.0001. Partitioning of trace elements into ostracod calcite is described by partition or distribution coefficients (K_D values), where $K_D[M] = (M/Ca_{shell})/M/Ca_{water})$, where M =

trace metal and M/Ca are atomic ratios. K_D[M] values, with certain caveats discussed below, tend to be constant for ostracod species or even genera. We used K_D[Sr] values of 0.22 for *Candona* (Keatings, 1999), 0.19 for *Prionocypris* (Holmes, unpublished data) and 0.17 for *Ilyocypris* (De Deckker, unpublished, in Holmes *et al*., 1992) to calculate Sr/Ca values for the Boxgrove Pond waters of 0.00174 ± 0.00043 (1s, n = 16). The inferred Sr/Ca_{water} values are slightly higher and more variable than those from Greywell, perhaps implying minor intermittent input of marine water to the ponds, although apart from this, the inferred Sr/Ca values from the Boxgrove Ponds are consistent with a chalk groundwater source. Using a simple two-component mixing model for seawater (Sr/Ca = 0.0088, Sr = 7.7 mg l^{-1}) and meteoric water (Sr/Ca = 0.0012, Sr = 0.3 mg l^{-1}) suggests a seawater percentage in the Boxgrove Pond of about 0.4 %.

The Sr-isotope values provide an additional tracer for water source, with the added advantage that Sr-isotopes are not fractionated between water and ostracod calcite (Reinhardt et al., 1999): the $^{87}Sr/^{86}Sr$ ratio of ostracod shell is thus the same as the ratio of the water in which it was formed. The $^{87}Sr/^{86}Sr$ ratio of ostracod shells from the Boxgrove Pond sediments is 0.70792 ± 0.00015 (1s) (Table 3), slightly higher than the value for Greywell water (0.70776 ± 0.00001, n = 4). The Sr-isotope values of the Boxgrove Ponds can be described using a similar two-component mixing model as for Sr/Ca ratios and the $^{87}Sr/^{86}Sr$ values also imply a small marine influence. Uncertainties in the $^{87}Sr/^{86}Sr$ ratios in both end members, however, lead to corresponding uncertainties in the mixing model (Fig. 5). The $^{87}Sr/^{86}Sr$ ratio of seawater may have been slightly lower during MIS13 (e.g. Farrell et al., 1995) compared with present. Moreover, the presence of a marine embayment close to Boxgrove may have altered the salinity and Sr isotope composition of seawater in

438 this area at that time, although $^{87}Sr/^{86}Sr$ ratios of marine ostracods from the Slindon
439 Sands (0.70914 ± 0.00003, n = 8: Darbyshire and Holmes in Roberts and Pope, in
440 press) are close to modern seawater values, suggesting that this was not the case.
441 Moreover, small variations in the composition of seawater end member have
442 negligible influence on the percentage of seawater in the Boxgrove Ponds inferred
443 from the Sr-isotope mixing model (Fig. 5). Potentially much larger variations in the Sr-
444 isotope ratio of the groundwater end member arise because the $^{87}Sr/^{86}Sr$ ratio of the
445 Campanian to Santonian age chalk in the area from which the groundwater would
446 have derived Sr varies from about 0.70744 to 0.70774 (McArthur et al., 2001). As
447 shown in Fig. 5, taking a best estimate of the Sr-isotope ratio of seawater of 0.70918
448 and allowing the composition of meteoric water to vary between the values quoted
449 above generates estimated seawater percentages in the Boxgrove Ponds of 0.7 and
450 1.8 %, slightly higher than the percentage calculated from Sr/Ca ratios.
451
452 Interestingly, both the Sr/Ca and $^{87}Sr/^{86}Sr$ ratios of individual ostracod samples from
453 the freshwater sediments show greater variability as well as slightly higher values
454 than those from the site at Greywell, which is unaffected by seawater. This variability
455 is further consistent with periodic inputs of seawater, perhaps through very minor
456 surface intrusion or sea spray, or of dried sea-salt aerosols. Despite uncertainties in
457 the figures however, it is clear that the marine influence on salinity was minor. The
458 Sr-isotope ratios in the foraminfera (0.70909 ± 0.00002, n = 5) (Table 3) are much
459 higher than those in the pond facies ostracods, yet similar to the marine ostracods
460 from the underlying Slindon sands, suggesting that they calcified in seawater before
461 being reworked from the underlying regressive shallow-marine facies that predate the
462 pond facies.
463

464 *4.4. Carbon isotopes*

465 The carbon isotope ratios of ostracods from the freshwater sediments reflect carbon
466 cycling within the waterbodies and their catchments. Fractionation of carbon from
467 dissolved inorganic carbon (DIC) into ostracod calcite has negligible temperature
468 control and appears to be an equilibrium process (Keatings et al, 2002). Assuming
469 the Boxgrove Ponds were largely groundwater fed, the carbon-isotope composition of
470 the DIC would have reflected that of groundwater. Carbon within the groundwater
471 would have been derived from two main sources, namely the Upper Chalk bedrock
472 and soil CO_2. The Upper Chalk has variable carbon isotope ratios, but values
473 typically lie between about +2 to +3 ‰ VPDB (Jarvis et al., 2006). The $\delta^{13}C$ value of
474 soil CO_2 lies between -34 and -24 ‰ in areas of C3 vegetation (Smith and Epstein,
475 1971; Deines, 1980). Assuming half of the DIC is derived from each of these two
476 sources, the groundwater $\delta^{13}C$ value would lie somewhere between about -16 and -
477 10.5 ‰, and calcite in equilibrium with that DIC would fall between about -15 and -9.5
478 ‰.
479
480 Two additional processes may modify the carbon isotope composition of the DIC.
481 First, exchange with atmospheric CO_2. This is a relatively slow process and complete
482 isotopic equilibrium is typically achieved only in water bodies with long residence
483 time. At complete isotopic equilibrium and a water temperature of 8 ˚C (the estimated
484 mean annual temperature at Boxgrove at this time), HCO_3^- is enriched in ^{13}C by 9.5
485 ‰ compared to CO_2 gas (Mook, 1986). Although we do not have measurements of
486 $\delta^{13}C$ values for MIS-13 CO_2, a pre-Holocene value of -6.5 ‰ (Leuenberger et al.,
487 1992) is probably a reasonable approximation. This would yield a $\delta^{13}C$ value in DIC
488 of +3‰ and in carbonate of +4 ‰. The ostracod values from the Boxgrove Ponds
489 (average ~-7.8 ‰) are much lower than this, suggesting that complete isotopic

490 equilibrium with the atmosphere was not achieved, implying that the residence time
491 of the ponds was short. Second, addition of ^{13}C-depleted carbon from respiration or
492 decay of aquatic plants will further reduce the $\delta^{13}C$ of the DIC (Deines, 1980).
493 Although the presence of *Chara* remains within the sediments and the ostracod
494 faunal assemblages themselves both testify to the existence of macrophytes within
495 the ponds, the observed $\delta^{13}C$ values within the ostracod shells can be explained
496 almost entirely by a groundwater source.
497
498 *4.5. Water isotopes*
499 The oxygen-isotope ratios of ostracod shells are controlled by the oxygen-isotope
500 ratio of the host water, calcification temperature and offsets from oxygen-isotope
501 equilibrium (vital offsets), which seem to be constant for individual genera or even
502 families. For candonids, the offset is well characterised as +2.2 ± 0.15 ‰ (von
503 Grafenstein et al., 1999). For *Prionocypris*, the other genus analysed here, there is
504 no published offset. However, values for paired analyses in the freshwater sediments
505 show no significant difference compared with *Candona* (mean difference = -0.05 ±
506 0.25, n = 7; Table 3). We therefore conclude that the vital offsets of both species are
507 about +2.2 ‰. We have used a bootstrap technique (Efron and Tibsharini, 1993) to
508 estimate the mean of the vital effect for *Prionocypris* as +2.15 with standard error ±
509 0.17 ‰ (Appendix A). The $\delta^{18}O$ values for the ostracods from the Boxgrove Pond
510 sediments fall within a fairly narrow range of -2.7 ± 0.24 for *Candona* and -2.8 ± 0.18
511 for *Prionocypris*, which equate to -4.9 and -5.2 ‰ for the two species, respectively, at
512 oxygen-isotope equilibrium.
513
514 To estimate the range of values that these data would imply for a hypothetical calcite
515 deposited in isotopic equilibrium with the pond waters, we first subtract the vital offset

for each species. We again used a bootstrap method, to generate an empirical distribution for $\delta^{18}O$ of equilibrium calcite, with a mean value of –4.93 and standard error of 0.16 ‰ on the PDB scale. We now use the estimated $\delta^{18}O$ values of equilibrium calcite for Boxgrove Ponds to reconstruct the oxygen-isotope ratio of meteoric precipitation at the site during the early Middle Pleistocene. To produce these reconstructions, we assume that the oxygen-isotope ratio of water in the shallow, groundwater-fed ponds with short residence time closely follows the weighted mean annual oxygen-isotope composition of local precipitation (Darling et al., 2003). The reconstruction of the past water-isotope composition of the Boxgrove Ponds from the ostracod values requires an estimate of past water temperature, for which we can use the MOTR- and MCR-derived reconstructions discussed above. Despite large differences between the reconstructed summer and winter air temperatures, ponds fed by shallow groundwater often show a small annual water temperature range that approximates the MAAT. At the Greywell site discussed above, for example, mean annual water temperature varied over a narrow range of less than 1 ˚C over a year, compared with air temperatures, which showed a ± 5.5 ˚C standard deviation over the same period. If the similarity between MAAT and water temperature also prevailed for the Boxgrove Ponds, the MOTR/MCR reconstructions of air temperature should provide a guide to likely water temperatures. The isotopic composition of the water itself can then be calculated from the temperature and the $\delta^{18}O$ of equilibrium calcite, using the equation of Kim and O'Neil (1997). For example, if the MAAT and water temperature were 8˚C, then the mean value of –4.93 ‰ VPDB for $\delta^{18}O$ of calcite at equilibrium would imply a water composition of $\delta^{18}O$ = -6.23 VSMOW. We have again employed a bootstrap re-sampling technique to combine the empirical distribution of $\delta^{18}O$ in equilibrium calcite with the distribution of values for MAAT implied by the combined ostracod-herptile mutual climatic range

(Fig. 4). Fig. 6 illustrates how the distributions of temperature and $\delta^{18}O$ of calcite are combined to produce an empirical distribution for possible values for $\delta^{18}O$ of pond water, representing the full range compatible with all the evidence from ostracod $\delta^{18}O$ measurements and the MOTR-MCR reconstructions.

Variation in the pond water temperature through the year could impart further uncertainty to the reconstructed water isotope values. However, the narrow range of $\delta^{18}O$ ostracod values from across several stratigraphic levels in the freshwater facies supports the contention that conditions were stable both seasonally and between years. *Candona neglecta* is a warm-season calcifier and, had water temperatures shown seasonal variation, would have reflected spring – summer temperatures. *Prionocypris zenkeri* in contrast is a year-round calcifier, yet its $\delta^{18}O$ values are similar to those for *C. neglecta* and show no greater variability. This suggests that the seasonal temperature range (recorded by *P. zenkeri*) was no greater than the inter-annual range of spring-summer temperatures (recorded by *C. neglecta*), and that both were small.

A final possible influence on the $\delta^{18}O$ composition of the ponds is marine input, since seawater has a higher $\delta^{18}O$ value than meteoric water. However, a marine contribution of ~2 % to the ponds, the maximum likely content, would only have the effect of raising their $\delta^{18}O$ value by about 0.2 ‰ and is therefore unlikely to have had a major influence in modifying freshwater values of a spring to a different composition in pond water. We have incorporated the range of calculated sea water contributions to the pond water into our bootstrap calculations (Appendix A), to yield the empirical distribution for $\delta^{18}O$ in the fresh water component (Fig. 6). This has mean –6.11 and

567 standard error ±0.19 ‰ SMOW and conforms moderately well to a normal
568 distribution (χ^2 = 17.14 with 9 d.f., p=0.046).
569
570 As discussed above, it is likely that the Boxgrove Ponds were supplied by
571 groundwater from a spring and/or seepage from the underlying Chalk aquifer. The
572 topography and structure of the Chalk aquifer precludes groundwater at Boxgrove
573 being derived from any source apart from local precipitation falling either very close
574 to the site itself or onto Chalk hills 100-200 m above sea level, within about 8 km
575 north of the site. Thus the fresh water compositions (Fig. 6) reflect palaeo-
576 groundwater originally derived from within a restricted area. In modern Europe
577 generally, the $\delta^{18}O$ value of locally derived groundwaters is close to that of average
578 or bulk composition of local meteoric precipitation, with only minor offsets between
579 them (Darling, 2004). The possible Middle Pleistocene thermal climates derived from
580 MOTR and MCR in the present study can all be found across western and central
581 Europe today, and in this region the differences between groundwaters and averaged
582 local precipitation are less than 0.5 ‰ $\delta^{18}O$ (Rozanski 1985; Darling et al. 2003;
583 Darling 2004). Thus, to a first approximation we may take our reconstructed $\delta^{18}O$
584 values for groundwaters feeding the Boxgrove Ponds to be equivalent to the average
585 $\delta^{18}O$ of local precipitation. Fig. 6 shows the modern values of $\delta^{18}O$ in local Chalk
586 groundwater (-6.5 ‰, based on a contour map in Darling et al., 2003) and in Chalk
587 groundwater and modern precipitation at Wallingford, 85 km north-northwest of
588 Boxgrove (-7.20, -7.28 ‰ respectively; Darling, 2004). The $\delta^{18}O$ of palaeo-water in
589 the Boxgrove Ponds was clearly ~1 ‰ heavier than modern precipitation at
590 Wallingford, but part of this difference may be due to a modern gradient in $\delta^{18}O$
591 between Wallingford and the south coast of England. There are no $\delta^{18}O$ data
592 available for precipitation at any site closer to Boxgrove (Darling and Talbot, 2003)

593 but the contoured difference in modern groundwater values is 0.7 ‰ heavier at
594 Boxgrove than Wallingford. In terms of the uncertainty of ±0.19 ‰ in the $\delta^{18}O$ of the
595 Boxgrove Pond water, a modern groundwater value of –6.5 ‰ lies two standard
596 errors from the best estimate of –6.11 ‰ , but this comparison takes no account of
597 uncertainty in the modern value. Overall, we draw the conclusion that the average
598 $\delta^{18}O$ of palaeo-precipitation on the south coast of England at the time the Slindon
599 Silts were deposited may have been up to ~0.4 ‰ heavier than modern precipitation,
600 but that this apparent difference is somewhat less than the overall uncertainties
601 involved. A stronger conclusion is that the early Middle Pleistocene precipitation was
602 not ^{18}O-depleted compared with modern precipitation.
603
604 *4.6. Mg/Ca ratios*
605 Mg partitioning from water into ostracod shells is temperature and species
606 dependent, but the temperature dependence of Mg partitioning into the shells of the
607 ostracod species analysed in this study is not known. However, we can compare the
608 Mg/Ca ratios of *Candona* at Slindon (Mg/Ca = 0.002) with values in the closely-
609 related species *C. candida* from Greywell (Mg/Ca = 0.011, water temperature = 11.8
610 ± 0.7 ˚C). Qualitatively, the results suggest lower water temperatures at Slindon
611 compared with Greywell, consistent with the MOTR air temperature reconstructions
612 discussed above. However, Mg/Ca ratios in ostracods are further complicated by
613 highly variable Mg partitioning in water with an Mg/Ca ratio ≤0.5 (Wansard *et al.*,
614 1998). Greywell waters have Mg/Ca ratio of 0.028 whereas Boxgrove Pond water
615 had unknown Mg/Ca. Although the latter was largely derived from chalk groundwater,
616 as discussed above, the small inputs of marine water may have changed the Mg/Ca
617 ratio sufficiently to have had a significant effect on Mg partitioning. Therefore,
618 although the Mg/Ca ratios of *C. neglecta* might imply that calcification temperature

619 was less than 12˚C, we cannot be certain of the magnitude of difference in the
620 absence of an independent indicator of Mg/Ca_{water}.
621
622 **5. Palaeoenvironmental implications and Conclusions**
623 Our multiproxy palaeoecological and geochemical data suggest that the landscape at
624 Boxgrove, during the time it was occupied by hominins in the early Middle
625 Pleistocene, supported a small lake or small, shallow, vegetated ponds that were
626 permanent, had short residence time and were fed by shallow chalk groundwater,
627 possibly from springs. Sedimentological evidence from the pond sediments suggests
628 that climatic cooling occurred sometime after the formation of the deposits that we
629 investigated in this study, perhaps associated with the downturn at the start of the
630 Anglian glaciation (MIS-12). This is consistent with our MOTR reconstructions, which
631 suggest colder winter and mean annual temperatures during the formation of the
632 pond sediments, although summer temperatures were similar to present. Mg/Ca
633 ratios in ostracods provide qualitative evidence for lower water temperatures in the
634 Boxgrove Ponds compared with likely modern values, although temperature
635 inferences must be viewed with caution since Mg partitioning would also have been
636 influenced by the water's Mg/Ca ratio.
637
638 Similarity between reconstructed oxygen-isotope values for precipitation from the
639 'pond facies' ostracods and present-day values is inconsistent with reduced air
640 temperatures during the early Middle Pleistocene interval that is the focus of our
641 study. They could be explained by a shift in seasonal precipitation regimes or a
642 change to a vapour source with a contrasting oxygen-isotope ratio compared to
643 present. Ostracod carbon isotope values are consistent with the ponds being mainly
644 groundwater fed and having a short residence time. Sr/Ca and Sr-isotope ratios in

ostracods from the pond facies confirm the ostracod faunal evidence for the ponds being freshwater, although there may have been a slightly marine influence, possibly from windborne sea spray.

The MCR reconstructions used in this paper have confirmed the data derived from other lines of evidence that the freshwater sediments were laid down at the end of a temperate stage. Although the vertebrate faunas are fully temperate, there are indications of increased continentality, as derived from the taxonomic habitat index (Roberts and Parfitt 1999), some cryophilic marine invertebrates (Whittaker 1999) and the presence of exotic rocks in the sediments of the Slindon Formation (Roberts and Pope in press). Additionally, there is little or no evidence for a hiatus, in the form of erosion or weathering profiles at the junction between the temperate and cold sediments, in the Boxgrove sequence thus indicating a relatively seamless and rapid climatic transition.

Our data illustrate the potential of combining ostracod geochemical and palaeoecological data for quantitative palaeoenvironmental reconstructions and provide information about the environment and climate of the Sussex Coastal Plain at a time when it was occupied by *H.* cf. *heidelbergensis*. Ostracod faunal assemblages can be used to inform on hydrological environment and, in favourable circumstances, to make quantitative estimates of past temperature using the MOTR method. Such reconstructions should ideally be verified using independent indicators, as we have done in this study using the herpetofauna. Although the reconstructed temperature ranges are quite large, they can be used to place useful constraints on those geochemical data that require independent estimates of temperature, especially oxygen isotopes. Mg/Ca ratios provide an additional palaeothermometer, although

671 quantitative reconstructions may be compromised by poor understanding of the
672 thermodependence of Mg uptake for individual species as well as complex effects of
673 water Mg/Ca ratio on Mg partitioning. Sr/Ca and Sr-isotope ratios provide information
674 about salinity in some circumstances: in coastal localities, this may reflect the
675 proportion of marine and meteoric water in a waterbody of mixed source origin.
676
677 **Acknowledgements**
678 Excavations at Boxgrove were funded by English Heritage. K. J. Sinka's work on
679 herptile MCR and investigations at Greywell by K. W. Keatings were both funded by
680 UK Natural Environment Research Council. We are grateful to R. I. Macphail, J.
681 Crowther, S. A. Parfitt and the late J. A. Holman for the use of unpublished data and
682 we thank C. Arrowsmith, H. Sloane (NIGL, Keyworth) and A. Osborn (UCL) for
683 analytical support, I. Boomer and an anonymous referee for constructive comments,
684 Miles Irving (UCL) for figure drafting and D. McCarroll for editorial support. NIGL
685 Publication number 774.
686
687
688 **Appendix A. Use of Bootstrap and Monte Carlo techniques for propagating**
689 **uncertainties in palaeoenvironmental reconstructions**
690 Palaeoenvironmental studies generate numerical data belonging to all types, from
691 nominal categories through ranked ordinal and interval scales to continuous real
692 numbers. The uncertainties associated with each element of data take equally varied
693 forms. Expressed forms of uncertainties may range from simple alternative possible
694 values or states (e.g. ‘forest’ or ‘grassland’), through probabilities assigned to these,
695 up to full confidence intervals around a value on a ratio scale. Combining such
696 different types of data to form estimated values for new variables, such as

$\delta^{18}O_{freshwater}$ in this paper, requires an adaptable technique for propagating uncertainties. The Bootstrap, in combination with Monte Carlo sampling methods that are closely related to it, provides the adaptability needed and is easy to implement using spreadsheet computer programs. Efron and Tibsharini (1993) and Davison and Hinckley (1997) provide introductions to bootstrap methods and their application.

The basic procedure in the Bootstrap technique is random re-sampling with replacement from a finite data set of *n* measured values, to generate a new set of *n* values known as a *bootstrap sample*. Because the random sampling involves replacement, it is usual for some of the *n* original values to be occur more than once in the bootstrap sample. This process is repeated a large number of times creating *N* bootstrap samples. Each sample is used to calculate a value for some statistic or quantity derived from the original data. A simple example is to find the mean for the *n* values in each bootstrap sample. Each calculated value is termed a *bootstrap replication* of the sample mean. Repetition generates *N* bootstrap replications, which together define an *empirical distribution function* (e.d.f.) of values for the mean. Because the e.d.f. is based on the original data, its average value provides a best-estimate for the mean of the population from which the data itself was a single sample. Furthermore, the standard deviation of the *N* replicates in the e.d.f. is an estimator for the standard error of the population mean.

Our initial application of the Bootstrap to the Slindon Silts provides an example. We measured $\delta^{18}O$ in paired specimens of *P.zenkeri* and *C.neglecta*, one pair from each of 7 separate sediment samples. Thus we had seven values for the difference in $\delta^{18}O$ between these species when they calcify their shells under what we assume

were identical conditions of temperature and $\delta^{18}O_{water}$. By sampling randomly and with replacement from the seven values, we created 1000 bootstrap samples and calculated the mean of each. Thus we obtained an e.d.f. for the mean difference, which had its own mean –0.045 and standard deviation 0.09 ‰. These are the best estimates of mean and standard error for the inter-species difference in $\delta^{18}O$.

The vital offset of *C. neglecta* is +2.2 ±0.15 ‰ (i.e. the fractionation of $\delta^{18}O$ between ostracod calcite and inorganically-formed calcite at isotopic equilibrium with the host water) (von Grafenstein *et al.*, 1999). The vital offset for *P. zenkeri* is not known, but if our assumption is correct that the paired specimens in the Slindon Silts experienced the same temperatures and $\delta^{18}O_{water}$, we can estimate it by adding the inter-species difference to von Grafenstein's value for *C. neglecta*. Using the mean values gives an estimate of +2.16 ‰ for *P. zenkeri*. To estimate the uncertainty we must convolute the e.d.f. for the mean inter-species difference with the uncertainty in *C. neglecta*'s vital offset. We assume that the latter is a normal distribution with standard deviation 0.15 ‰. We began by generating 1000 random values from the *C.neglecta* error distribution. Each of these was paired with a value selected at random from the bootstrapped e.d.f. for inter-species difference. The result of adding together the members of each pair is 1000 estimated values for the vital offset of *P.zenkeri*, i.e. a new e.d.f. for this vital offset. The mean and standard deviation of this e.d.f. are the best estimate and error for the vital offset of *P. zenkeri*, +2.16 ± 0.18 ‰.

While the estimation of uncertainty in the inter-species difference is a simple example of the Bootstrap applied to a single variable, the calculation of *P. zenkeri*'s vital offset adds a Monte Carlo approach. Monte Carlo samples are drawn singly from an e.d.f.

749 or from an assumed probability density function (p.d.f.). In this case, the pairs of
750 values needed for each replication were drawn respectively from an assumed normal
751 distribution for the *C. neglecta* vital offset, and from a bootstrapped e.d.f. for the
752 inter-species difference.
753
754 We used a further elaboration of Monte Carlo and Bootstrap procedures in estimating
755 the $\delta^{18}O_{equilibrium}$ for calcite formed in isotopic equilibrium with the water that hosted
756 the ostracods. We have 11 measurements of $\delta^{18}O$ in *C. neglecta* and 7 in *P. zenkeri*.
757 We first adjusted the *P. zenkeri* values to remove the systematic inter-species
758 difference, then subtracted the vital offset for *C. neglecta* from the ostracod values of
759 both species. Bootstrap resampling was used to create 1000 bootstrap samples,
760 each of 18 values drawn from the 18 ostracod measurements with replacement.
761 Prior to each resampling, the *P. zenkeri* values were individually adjusted by adding
762 a value randomly selected from the e.d.f of mean inter-species difference that had
763 been previously generated. By applying this Monte Carlo adjustment before each
764 bootstrap replication the ostracod data are adjusted to a common mean, and at the
765 same time the uncertainty in the average difference between species is propagated.
766 We then subtracted from every element of each bootstrap sample an individual
767 value for the vital effect of *C. neglecta*, drawn by Monte Carlo sampling from a
768 normal distribution with von Grafenstein's mean of +2.2 ± 0.15 ‰ standard deviation.
769 This step produced a bootstrap sample of 18 values of $\delta^{18}O_{equilibrium}$ for a hypothetical
770 calcite formed in isotopic equilibrium with the same water as the ostracods.
771 Calculating the mean of these 18 values, and repeating for all 1000 repetitions,
772 produced an e.d.f. for the average $\delta^{18}O_{equilibrium}$, with mean and standard deviation of
773 -4.93 ±0.16 ‰ PDB.
774

To calculate the $\delta^{18}O$ of pond water we used the equation of Kim and O'Neil (1997) for the equilibrium fractionation of oxygen isotopes between calcite and water as a function of temperature, $1000.\ln\alpha_{\mathbf{calcite\text{-}H2O}} = 18{\cdot}03.1000/T - 32{\cdot}42$, with T = temperature (K) and $\alpha_{\mathbf{calcite\text{-}H2O}} = (1000 + \delta^{18}O_{calcite})/(1000 + \delta^{18}O_{H2O})$. If values for T and $\delta^{18}O_{calcite}$ are assumed, the equation can be solved to give $\delta^{18}O_{H2O}$. Preliminary conversion of $\delta^{18}O_{calcite}$ from the PDB to the SMOW scale is required, using $\delta^{18}O_{SMOW} = 1{\cdot}03086\ \delta^{18}O_{PDB} + 30.86$ (Criss, 1999, p.33).

Our estimates for T come from the combined ostracod-herptile reconstruction of MAAT by the MOTR-MCR method. Figs.4 and 4C of the main paper show that the combined MCR occupies part of a two-dimensional space that is gridded at integer values of the climate variables on both axes. The true climate lies within this range and we assume that every grid intersection has the same probability of representing it, i.e. the attribute 'true climate' has a uniform *a priori* probability of 1/G at all intersections within and on the boundary of the mutual range, where G is the number of such intersections, and a zero probability outside the mutual range. (This assumption has been questioned and various approaches to identifying a 'most probable' value for the climate have been suggested by Atkinson et al. 1987, Sinka 1993, Dockerty and Lovett 2003, Dockerty et al. 2003, Bray et al. 2006 and Horne and Mezquita 2008. Such modifications rest upon complex and problematic assumptions and will not be discussed here. As far as the Bootstrap-Monte Carlo methodology is concerned, it would be easy to incorporate them.) The combined ostracod-herptile MCR (Fig. 4C) has 48 grid intersections, so G = 48, and each intersection has an estimated MAAT defined by $(T_{MAX} - T_{RANGE}/2)$. The frequency distribution of MAAT among these 48 cases is shown in Fig. 6B. Note that because it

800 is gridded, MAAT is interval data, so does not possess a continuous uncertainty
801 distribution.
802
803 To generate an e.d.f. for $\delta^{18}O_{pondwater}$ we adopted a Monte Carlo approach. A value
804 from the list of 48 MAATs was selected at random and combined with a value drawn
805 at random from the e.d.f. of $\delta^{18}O_{equilibrium}$ already generated. The pair of values was
806 then used to generate a value for $\delta^{18}O_{pondwater}$ by inserting MAAT for T and
807 $\delta^{18}O_{equilibrium}$ for $\delta^{18}O_{calcite}$ in the Kim and O'Neil equation above. This was repeated
808 to create 1000 replications. As a further part of each replication, allowance was
809 made for the seawater component of the pond water. Section 4.3 of the main paper
810 derives three estimates for the seawater component in the ponds, namely 0.4, 0.7
811 and 1.8 %. We assumed these to each have a probability of 1/3 and made a random
812 selection from them for each replication. The chosen value was used to calculate the
813 $\delta^{18}O_{freshwater}$ of the fresh water component, by assuming simple mixing with sea water
814 with $\delta^{18}O_{seawater}$ = 0 ‰SMOW.
815
816 These procedures gave rise to an e.d.f. for $\delta^{18}O_{freshwater}$ with mean of -6.11 and
817 standard deviation of 0.19 ‰ SMOW, shown in Fig. 6B of the main paper. A Chi-
818 square test of fit to a normal distribution gave χ^2 =17.14 with 9 degrees of freedom,
819 indicating a probability of 4.6% that the e.d.f. was a sample drawn from a normal
820 distribution with the same mean and standard deviation. Thus, the e.d.f. is not a very
821 close fit to a normal curve, despite the visual resemblance in Fig. 6B.
822
823 This detailed example illustrates the adaptability and power of combining Bootstrap
824 and Monte Carlo methods to propagate uncertainties from the mixed data types

825 commonly encountered in palaeoenvironmental reconstructions. The present
826 example has included interval data (sea water percentage, MAAT), ratio data ($\delta^{18}O$ of
827 ostracods) and parametric data (vital offset for *C. neglecta*). A further advantage of
828 using these simple techniques is that implementing them helps the investigator to
829 identify explicitly the assumptions that are being made, and thus to consider their
830 justification.
831
832 **References**

833 Atkinson, T.C., Briffa, K.R., Coope, G.R., 1987. Seasonal temperatures in Britain
834 during the past 22,000 years, reconstructed using beetle remains. Nature
835 315, 587-592.

836 Atkinson, T.C., Briffa, K.R., Coope, G.R., Joachim, M.J., Perry, D.W., 1986. Climatic
837 calibration of coleopteran data. Chapter 41 in Berglund, B.E. (ed.) Handbook
838 of Holocene Palaeoecology and Palaeohydrology. Chichester, J.Wiley & Sons,
839 851-858.

840 Barnes, R.S.K., 1980. Coastal Lagoons. Cambridge, Cambridge University Press.
841 106pp.

842 Birck, J. L., 1986. Precision K-Rb-Sr Isotopic Analysis - Application to Rb-Sr
843 Chronology. Chemical Geology 56**,** 73-83.

844 Bray, P.J., Blockley, S.P.E., Coope, G.R., Dadswell, L.F., Elias, S.A., Lowe, J.J.,
845 Pollard, A.M., 2006. Refining mutual climatic range (MCR) quantitative
846 estimates of palaeotemperature using ubiquity analysis. Quaternary Science
847 Reviews 25, 1865-1876.

848 Criss, R.E., 1999. Principles of Stable Isotope Distribution. New York & Oxford,
849 Oxford University Press, 254pp.

850 Darling, W.G., 2004. Hydrological factors in the interpretation of stable isotopic proxy
851 data present and past: a European perspective. Quaternary Science Reviews
852 23, 743-770.

853 Darling, W.G., Talbot, J.C., 2003. The O & H stable isotope composition of fresh
854 waters in the British Isles. 1. Rainfall. Hydrology & Earth System Sciences 7,
855 163-181.

856 Darling, W.G., Bath, A.H., Talbot, J.C., 2003. The O & H stable isotopic composition
857 of fresh waters in the British Isles. 2. Surface waters and groundwater.
858 Hydrology and Earth System Sciences 7,183-195.

859 Davison, A.C., Hinckley, D.V., 1997. Bootstrap Methods and their Application.
860 Cambridge, Cambridge University Press, 582pp.

861 De Deckker, P., 1981. Ostracods of athalassic saline lakes - A review. Hydrobiologia
862 81, 131-144.

863 Deines, P. 1980. The isotopic composition of reduced organic carbon. In: Fritz, P.,
864 Fontes, J. C. (Eds.), Handbook of Environmental Isotope Geochemistry,
865 Amsterdam, Elsevier Scientific Publishing Company, pp. 329-406.

866 Dockerty, T., Lovett, A., 2003. A location-centred, GIS-based methodology for
867 estimating the potential impacts of climate change on nature reserves.
868 Transactions in GIS 7, 345-70.

869 Dockerty, T., Lovett, A., Watkinson, A., 2003. Climate change and nature reserves:
870 examining the potential impacts, with examples from Great Britain. Global
871 Environmental Change 13, 125-135.

872 Efron, B., Tibsharini, R. J., 1993. An Introduction to the Bootstrap. London,
873 Chapman & Hall, 436pp.

874 Farrell, J.W., Clemens, S.C., Grommet, L.P., 1995. Improved chronostratigraphic
875 reference curve of late Neogene seawater $^{87}Sr/^{86}Sr$. Geology 23, 403-406.

876 Griffiths, H. I., Holmes, J. A., 2000. Non-marine ostracods and Quaternary
877 palaeoenvironments. Quaternary Research Association Technical Guide 8,
878 179pp.

879 Holman, J. A. 1999. Herpetofauna. In, Roberts, M.B., Parfitt, S.A. (Eds) Boxgrove. A
880 Middle Pleistocene hominid site at Eartham Quarry, Boxgrove, West Sussex.
881 London: English Heritage Archaeological Report 17, London, English Heritage,
882 pp.181-187.

883 Holmes J. A., Hales P. E., Street-Perrott F. A., 1992. Trace-element chemistry of
884 non-marine ostracods as a means of palaeolimnological reconstruction: an
885 example from the Quaternary of Kashmir, northern India. Chemical Geology
886 95, 177-106.

887 Holmes, J. A., Chivas, A. R. 2002. Ostracod shell chemistry - overview. In: Holmes,
888 J. A., Chivas, A. R. (Eds.), The Ostracoda: Applications in Quaternary
889 Research, American Geophysical Union Geophysical Monograph. Washington
890 DC, American Geophysical Union, pp. 183-204.

Horne, D. J., 2007. A mutual temperature range method for Quaternary palaeoclimatic analysis using European nonmarine Ostracoda. Quaternary Science Reviews 26, 1398-1415.

Horne, D. J., Mezquita, F., 2008. Palaeoclimatic applications of large databases: developing and testing methods of palaeotemperature reconstruction using nonmarine otracods. Senckenbergiana Lethaea 88, 93-112.

Jarvis, I., Gale, A. S., Jenkyns, H. C., Pearce, M. A., 2006. Secular variation in Late Cretaceous carbon isotopes: a new delta C-13 carbonate reference curve for the Cenomanian-Campanian (99.6-70.6 Ma). Geological Magazine 143, 561-608.

Keatings, K.W., 1999. The basis for ostracod shell chemistry in palaeoclimate reconstruction. Unpublished PhD thesis, Kingston University.

Keatings, K.W., Heaton, T.H.E., Holmes, J.A., 2002. Carbon and oxygen isotope fractionation in non-marine ostracods: Results from a 'natural culture' environment. Geochimica et Cosmochimica Acta 66, 1701-1711.

Kim, S. T., and O'Neil, J. R., 1997. Equilibrium and nonequilibrium oxygen isotope effects in synthetic carbonates. Geochimica et Cosmochimica Acta 61, 3461-3475.

Leuenberger, M., Siegenthaler, U., Langway, C.C., 1992. Carbon isotope composition of atmospheric CO_2 During the last ice-age from an Antarctic Ice core. Nature 357, 488-490.

McArthur, J. M., Howarth, R. J., Bailey, T. R., 2001. Strontium isotope stratigraphy:

913 LOWESS version 3: Best fit to the marine Sr-isotope curve for 0-509 Ma and
914 accompanying look-up table for deriving numerical age. Journal of Geology
915 109, 155-170.

916 Meisch, C., 2000. Freshwater Ostracoda of western and central Europe.
917 Süßwasserfauna von Mitteleuropa 8/3. Stuttgart, Gustav Fischer, 522pp.

918 Mook, W. G., 1986. ^{13}C In atmospheric CO_2. Netherlands Journal of Sea Research
919 20, 211-223.

920 Murray, J. W., 1979. British Nearshore Foraminiferids. Synposes of the British Fauna
921 (New Series), 16. London, Academic Press.

922 Pitts, M.W., Roberts, M.B. 1997. Fairweather Eden: Life in Britain half a million
923 years ago as revealed by the excavations at Boxgrove. London, Century.
924 356pp.

925 Reinhardt E. G., Blenkinsop J., Patterson R. T., 1999. Assessment of a Sr isotope
926 vital effect (Sr-87/Sr-86) in marine taxa from Lee Stocking island, Bahamas.
927 Geo-Marine Letters 18, 241-246.

928 Roberts, M.B., Parfitt, S.A. 1999. Boxgrove. A Middle Pleistocene hominid site at
929 Eartham Quarry, Boxgrove, West Sussex. London, English Heritage
930 Archaeological Report 17. 456pp.

931 Roberts, M.B., Pope, M.I., in press. Mapping the early Middle Pleistocene deposits
932 of the Slindon Formation, across the coastal plain of West Sussex and eastern
933 Hampshire, UK. London, Left Coast Press.

934 Roberts, M.B., Stringer, C.B., Parfitt, S.A., 1994. A hominid tibia from Middle
935 Pleistocene sediments at Boxgrove, UK. Nature 369, 311-313.

936 Robinson, J. E. 1998. Ostracoda, In: Preece, R. C., Bridgland, D. R. (Eds.), Late
937 Quaternay Environmental Change in North-west Europe: Excavations at
938 Holywell Coombe, Southeast England. London, Chapman and Hall, pp. 242-
939 253.

940 Rozanski, K., 1985. Deuterium and oxygen-18 in European groundwaters – links to
941 atmospheric circulation in the past. Chemical Geology (Isotope Geoscience
942 Section) 52, 349-363.

943 Sinka, K.J., 1993. Developing the Mutual Climatic Range Method of Palaeoclimatic
944 Reconstruction. Unpublished Ph.D. Thesis, University of East Anglia, 2 vols.,
945 212pp & 136pp.

946 Sinka, K.J., Atkinson, T.C., 1999. A mutual climatic range method for reconstructing
947 palaeoclimate from plant remains. Journal of the Geological Society, London
948 156, 381-396.

949 Smith, A. J., Horne, D. J. (2002). Ecology of marine, marginal marine and nonmarine
950 ostracodes. In: Holmes, J. A., Chivas, A. R. (Eds.), The Ostracoda:
951 Applications in Quaternary Research, American Geophysical Union
952 Geophysical Monograph. Washington DC, American Geophysical Union, pp.
953 37-64.

954 Smith, B. N., Epstein, S. 1971. Two categories of $^{13}C/^{12}C$ ratios for higher plants.
955 Plant Physiology 47, 380-384.

956 von Grafenstein U., Erlernkeuser H., Trimborn P., 1999. Oxygen and carbon isotopes
957 in modern fresh-water ostracod valves: assessing vital offsets and
958 autecological effects of interest for palaeoclimate studies. Palaeogeography
959 Palaeoclimatology Palaeoecology 148, 133-152.

960 Wansard G., De Deckker P., Julià R. (1998) Variability in ostracod partition
961 coefficients D(Sr) and D(Mg) implications for lacustrine palaeoenvironmental
962 reconstructions. Chemical Geology 146, 39-54.

963 Whatley, R., 1988. Population structure of ostracods: some general principles for the
964 recognition of palaeoenvironments.In De Deckker, P., Colin, J. -P. and
965 Peypouquet, J. -P., (Eds.), Ostracoda in the Earth Sciences, Amsterdam,
966 Elsevier, pp. 245-256.

967 Whittaker, J. E., 1999. Foraminifera and Ostracoda, In: Roberts, M. B., Parfitt, S. A.
968 (Eds.), Boxgrove: A Middle Pleistocene hominid site at Eartham Quarry,
969 Boxgrove, West Sussex. Archaeological Report, 17, London, English Heritage,
970 pp. 163-170.

971

971 **Figures**

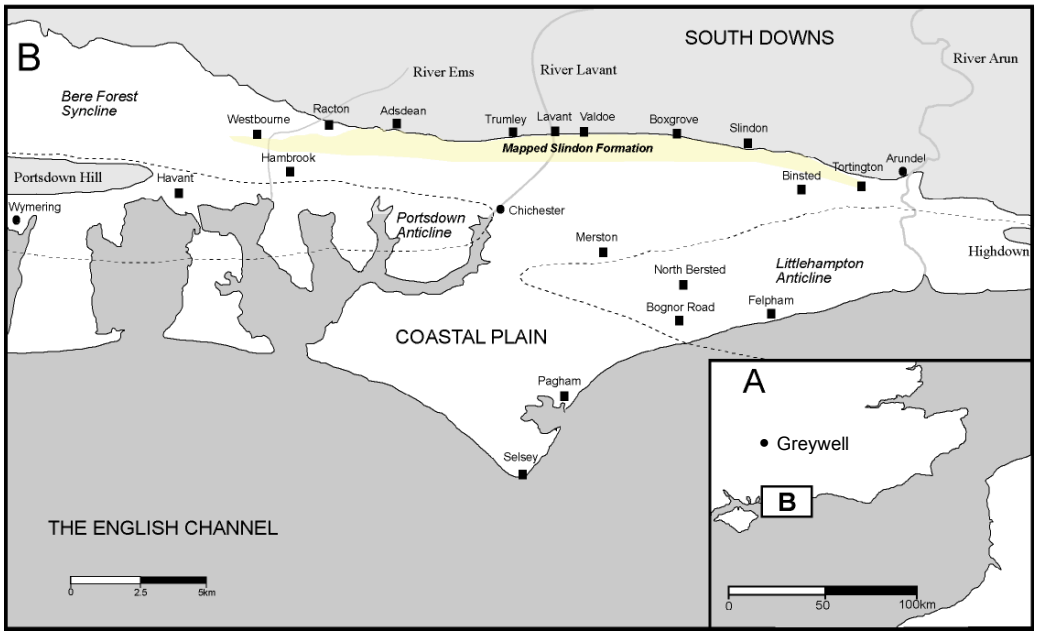

972

C

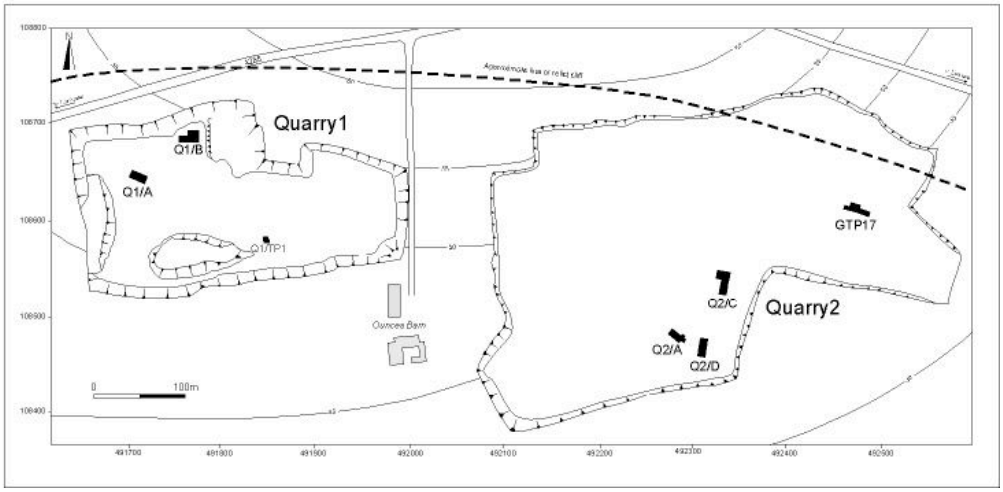

973

974

975 Fig. 1. Location map. A. Location of the Sussex coastal plain and Greywell. B.

976 Location of Eartham Quarry, at Boxgrove, and other sites on the Sussex coastal plain

977 C. Plan of quarries at Eartham.

978

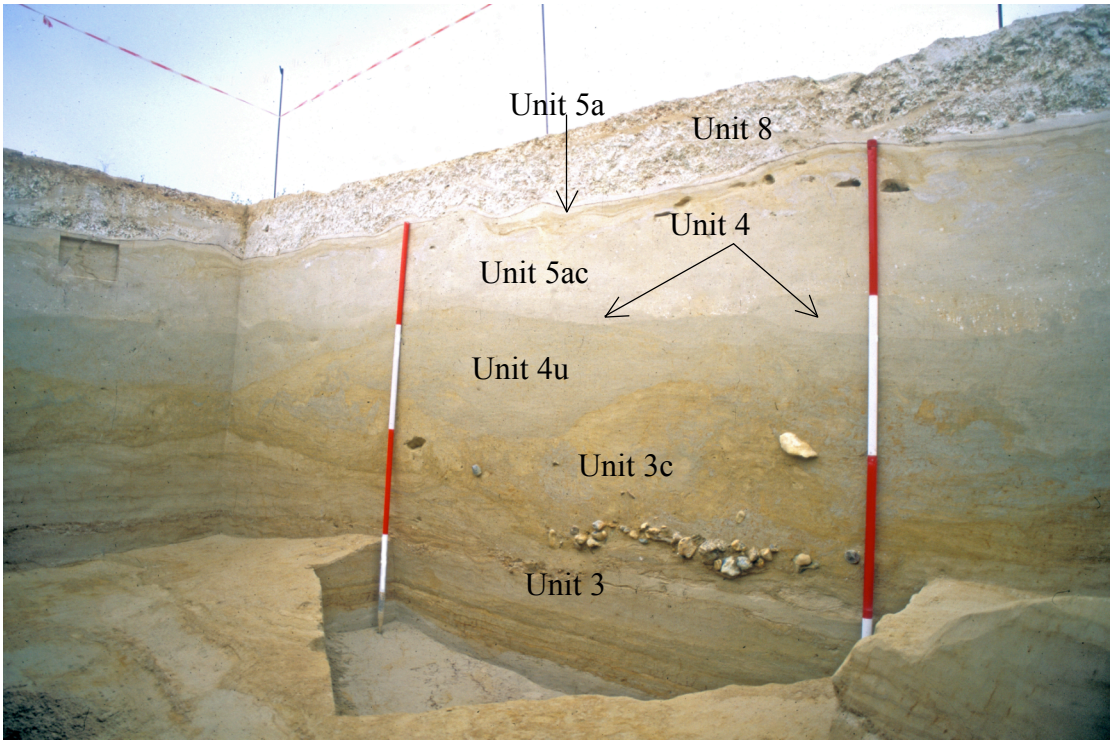

979

980

981

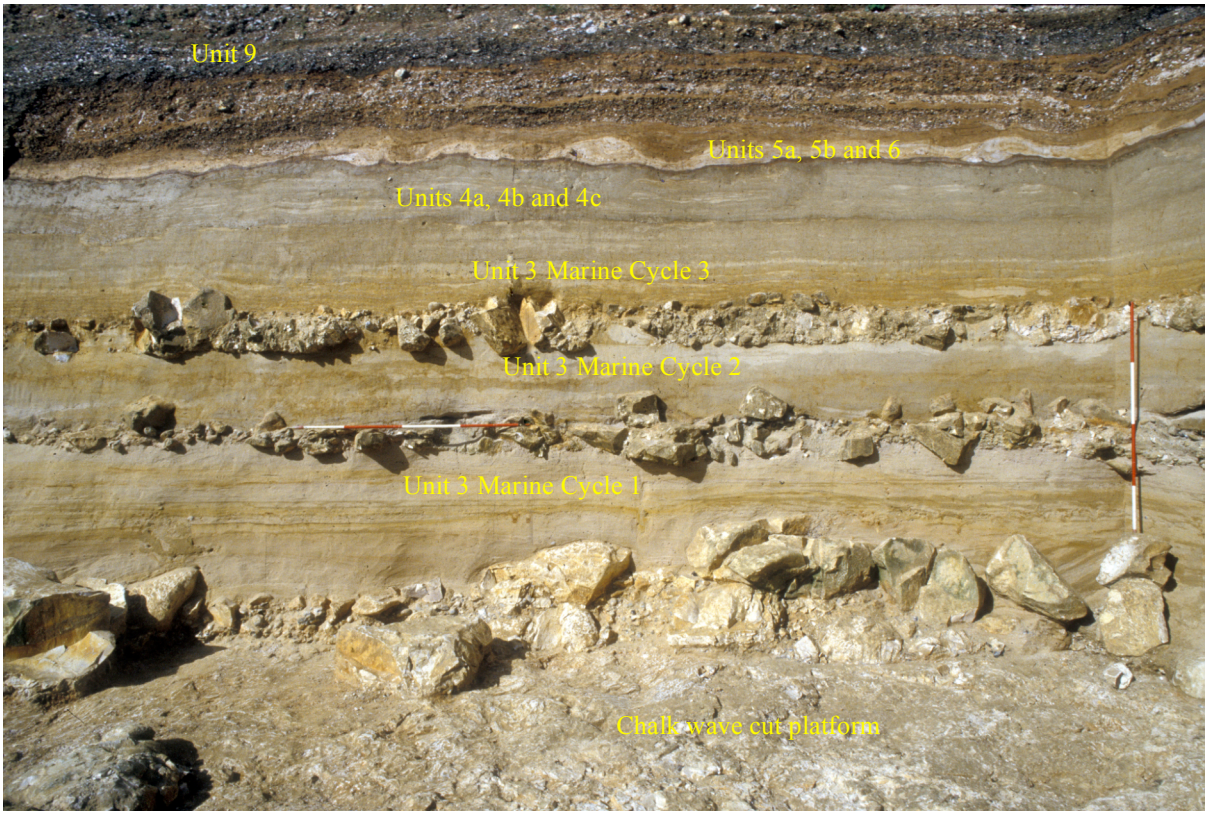

982

983

Fig. 2. A. The marine/freshwater/terrestrial sequence at Q1/B Trench 23 showing the channel and its associated infill (Unit 3c), cutting through the marine Slindon Sand (Unit 3). The channels deposits are overlain by the freshwater sediments of Units 4u and 5ac. Note the presence of the mineralised organic horizon Unit 5a, which completely covers the freshwater deposits at this part of the site (Scales in 0.50 metre divisions). B. The marine/terrestrial sequence at the Boxgrove type section Q2/GTP13 (Table 1). The lower two debris bands are the seaward ends of beaches and the upper, between marine Cycles 2 and 3. is a debris flow from cliff collapse (Scales in 0.5 metre divisions).

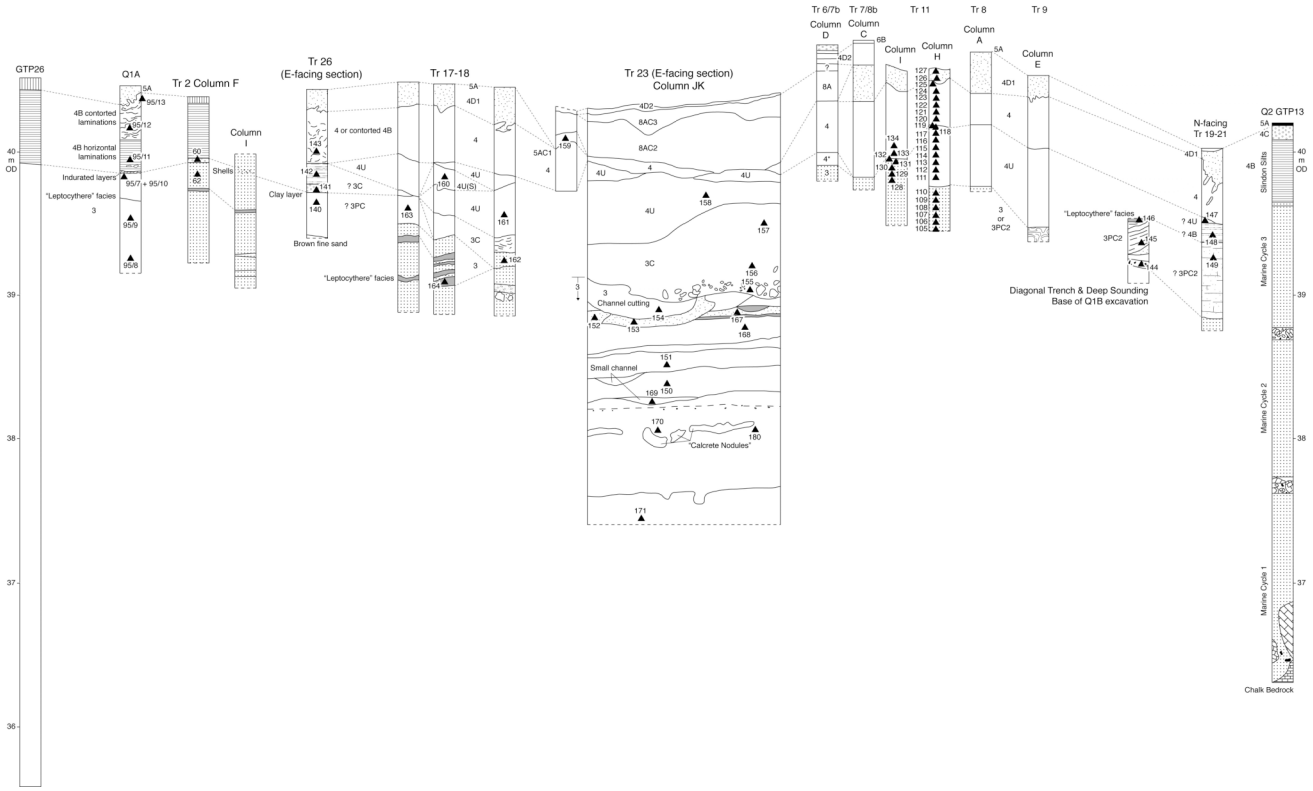

Fig. 3. Location of samples taken from Quarry 1/B. Samples from which microfossils were analysed for isotopes and/or trace elements are listed in Table 3.

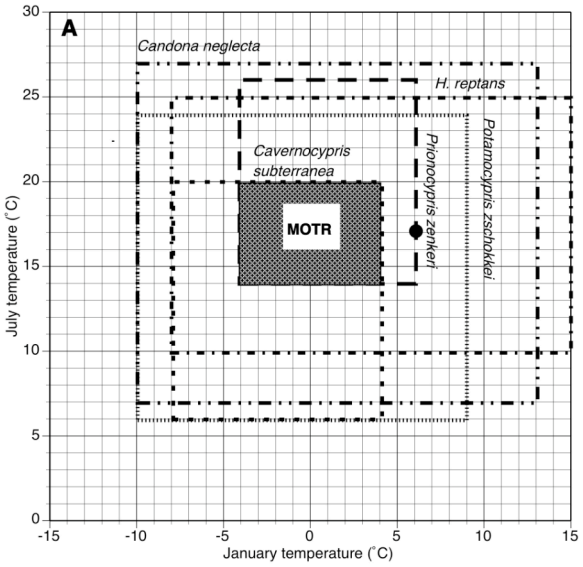

1021

1022

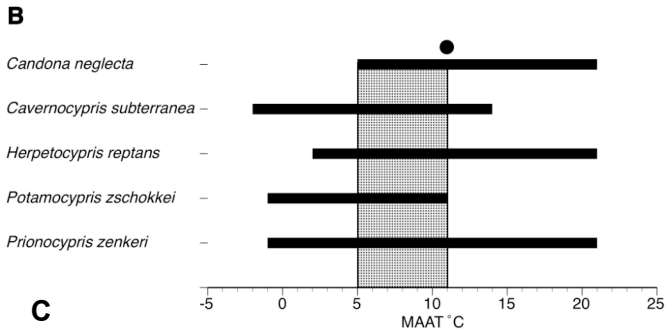

1023

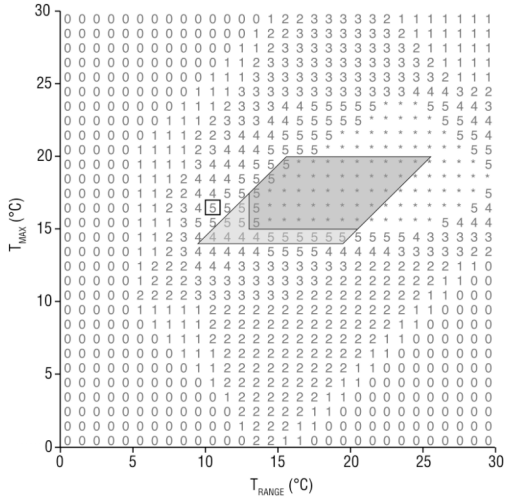

1024

1025

1026

1027

1028

1029 Fig. 4. Temperature reconstructions for the Slindon Silts ‘pond facies’. (A) maximum
1030 and minimum January and July air-temperature ranges and (B) mean annual air
1031 temperature ranges, for the occurrences of ostracod taxa found in Units 3c, 4u and
1032 4u(s) of the Slindon Silts freshwater facies using the MOTR method. In both figures,
1033 filled circle denotes present-day instrumental temperatures from Eastbourne. (C)
1034 Mutual climate range estimates of T_{MAX} and T_{RANGE} based on the six herptile species
1035 found in the Slindon Silts freshwater facies as presented in Sinka (1993). The
1036 numbers on the graph represent the number of the six species present in each 1˚C
1037 interval of T_{MAX} and T_{RANGE} space. The asterisks represent intervals in which all six
1038 species where found. The shaded parallelogram represents the reconstructed
1039 ostracod MOTR; the dark-shaded area is the combined herptile MCR – ostracod
1040 MOTR reconstruction that is used in the oxygen isotope calculation described in the
1041 text. The small bold square represents present-day instrumental temperatures from
1042 Eastbourne
1043
1044
1045

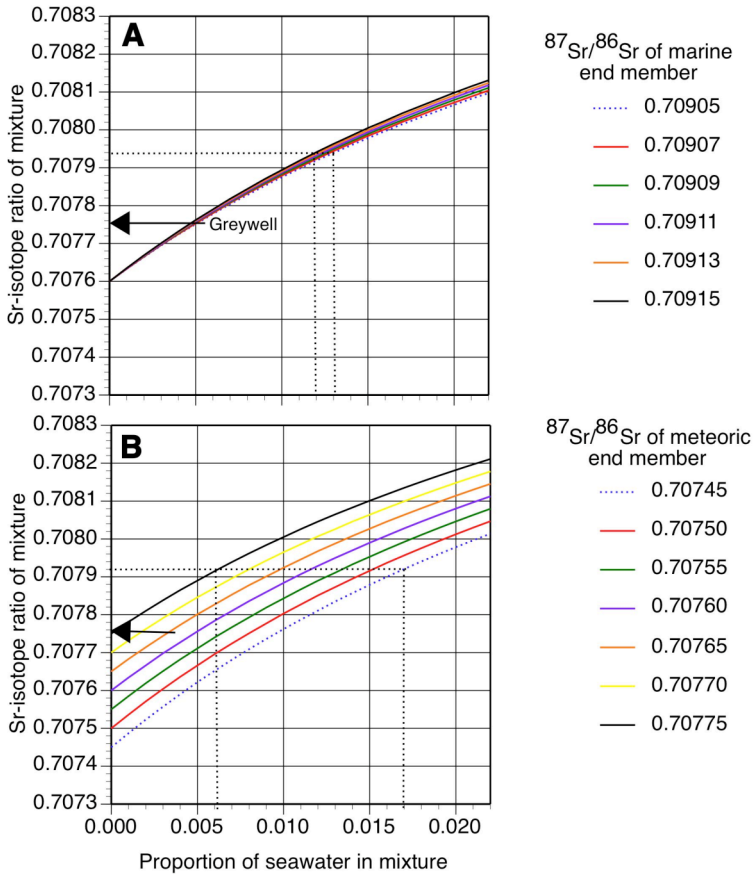

Fig. 5. Sensitivity of $^{87}Sr/^{86}Sr$ ratios of Boxgrove Pond water to varying proportions of seawater and differing $^{87}Sr/^{86}Sr$ ratios of A the marine end member and Bthe meteoric end member. In A, the $^{87}Sr/^{86}Sr$ ratios of the meteoric end member is set to 0.70760 and the ratio of the marine end member varied between 0.70905 and 0.70915. In B, the $^{87}Sr/^{86}Sr$ ratio of seawater is set to 0.7091 and the ratio of the meteoric end member varied between 0.70745 and 0.70775, the likely range of values in the upper chalk bedrock from which the shallow groundwater would have derived Sr. In both graphs, the dotted lines link the Sr-isotope ratios of the Boxgrove Pond waters, inferred from the ostracod values, with the possible range in proportion of seawater given the variability in end member composition in each case. From these graphs, it can be seen that the reconstructions of marine input to the ponds are relatively insensitive to the $^{87}Sr/^{86}Sr$ ratio of the marine end member, but much more sensitive to the composition of the meteoric end member

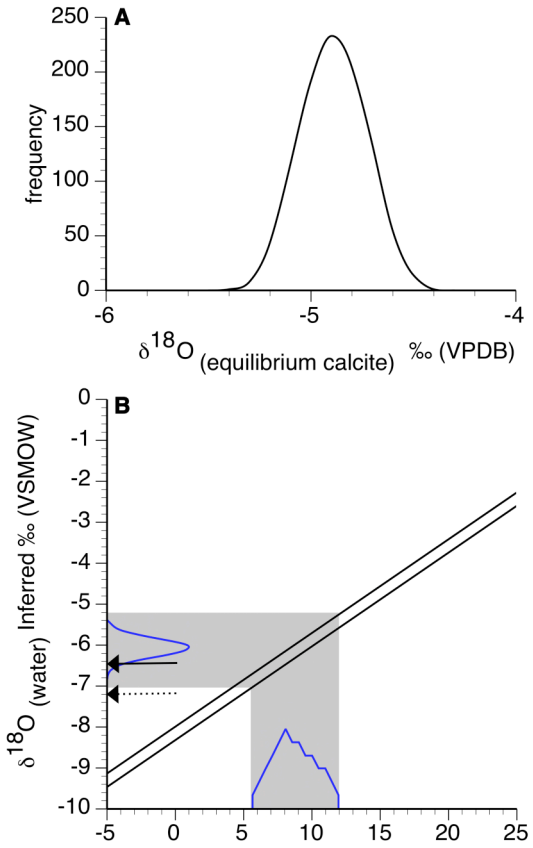

1060

1061

1062 Fig. 6. A. Bootstrap distribution of 1000 replications of 18 values of $\delta^{18}O_{equilibrium}$ for a
1063 hypothetical calcite formed in isotopic equilibrium with the same water as the
1064 ostracods. The mean and standard deviation are -4.93 ±0.16 ‰ PDB. B. Inferred
1065 $\delta^{18}O$ values of Boxgrove Pond water from $\delta^{18}O$ values of ostracod shells from the
1066 Slindon Silts freshwater sediments, adjusted for vital offsets as discussed in the text.
1067 Lines are water isotope compositions (plus and minus one standard deviation around
1068 the mean of the bootstrap $\delta^{18}O$ values) calculated from ostracod shells adjusted for
1069 vital offsets. Arrows mark the approximate $\delta^{18}O$ value of modern local groundwater
1070 (solid arrow, estimated from the maps in Darling et al. 2003) and groundwater at
1071 Wallingford, Oxfordshire (dashed arrow; Darling et al. 2003). Water temperature
1072 ranges are mean annual values inferred from MOTR and MCR.

1073

1081 Table 1. Stratigraphic relationship between the standard Boxgrove sequence and
1082 that recorded at Quarry 1/B (Q1/B), the spring fed pond. Unit 4c and its
1083 chronostratigraphic correlatives are outlined in black and shaded. Unit 7 is a
1084 sedimentary unit that is in continuous formation until the burial of the cliff by mass
1085 movement deposits. (Not to scale).

Member	Description and Interpretation		Standard	Q1/B	Description and Interpretation
Eartham Upper Gravel	Calcareous Head. Mass movement deposit.		Unit 10	Unit 10	Calcareous Head. Mass movement deposit.
Eartham Lower Gravel	Path gravel. Freeze thaw sorted flint gravel.		Unit 9		
	Chalk pellet gravel. Waterlain, weathered and sorted chalk clasts.		Unit 8	Unit 8	Chalk pellet gravel. Dewatering structures initiated.
	Cliff collapse.	Unit 7	Unit 7		
	Calcareous muds/brickearth. Colluvial and waterlain silts.		Units 5b, 6	Unit 6b	Calcareous muds/brickearth. Colluvial and waterlain silts.
Slindon Silt	Mineralised and compressed organic deposits. Alder/fen carr.		Unit 5a	Unit 5a	Mineralised and compressed organic deposits. Alder/fen carr.
	Soil horizon developed on top of the silts. Polder type soil.		Unit 4c	4d2, 4d3, 5ac	Spring discharge sediments with colluvial input towards the top (5ac)
	Intertidal laminated muds laid down in a semi-enclosed marine bay.		Unit 4b	Unit 4d1	Spring discharge sediment. Intraformational calcretes.
				Unit 4	Massive silt from freshwater reworking of Units 4a and 4b. Heavily deformed.
			Unit 4a	Unit 4u	Massive fine silt from freshwater reworking of Units 4a and 4b.
Slindon Sand	Near-shore marine sands.		Unit 3	Units 3/4, 3c	Freshwater channels and freshwater scoured landsurface, from springs at cliff base.
				Unit 3	Nearshore marine sands with a truncated upper surface.

1086
1087
1088
1089
1090
1091
1092
1093
1094
1095
1096
1097
1098

1099 Table 2. Habitat affinities and water chemistry preferences for ostracod species from
1100 the sediments of the Slindon Silts freshwater facies (from information in De Deckker,
1101 1981; Meisch, 2000).

Species	Maximum salinity tolerance	Habitat preferences
Herpetocypris reptans	15.7 ‰	Permanent waterbodies of all sizes together with sluggish streams; often associated with dense vegetation and mud substrate; often associated with *Chara*
Candona neglecta	15.7 ‰	Found in small ponds and in springs and streams; burrows into soft, organic, mud
Prionocypris zenkeri	not known	Found in gently-flowing streams, with rich aquatic vegetation, often connected to springs; often associated with *Chara*
Ilyocypris bradyi	6.4 ‰	Found in slow-flowing waters and springs, and spring-fed ponds; lives on mud substrates and aquatic vegetation
I. quinculminata	5 ‰ (*I. monstrifica*)	Extinct, but possibly related to *I. monstrifica*, which is associated with organic muddy substrates and slow-flowing water
Cavernocypris subterranea	not known	Associated with both surface and underground waters, springs, spring-fed streams and the littoral zone of spring-fed ponds and lakes
Potamocypris zshokkei	not known	Associated with slow-flowing springs, spring-fed ponds and spring-fed streams

1102
1103
1104
1105
1106
1107
1108
1109
1110
1111

Table 3. Geochemical data relating to ostracod shells and foraminiferal tests from the Slindon Silts freshwater facies.

Quarry/Trench/Column	Level	Unit	Species	Mg/Ca	Sr/Ca
Q1/B Tr11E Col H	MP113	4u	*P. zenkeri*	0.00155	0.00030
Q1/B Tr11E Col H	MP113	4u	*Candona neglecta*	0.00256	0.00046
Q1/B Tr11E Col H	MP113	4u	*Ilyocypris bradyi*	0.00136	0.00019
Q1/B Tr11E Col I	MP132	4u	*P. zenkeri*	0.00107	0.00030
Q1/B Tr11E Col I	MP132	4u	*Candona neglecta*	0.00212	0.00034
Q1/B Tr11E Col I	MP132	4u	*Ilyocypris bradyi*	0.00157	0.00016
Q1/B Tr11E Col H	MP114	4u	*C. neglecta*	0.00210	0.00041
Q1/B Tr11E Col H	MP114	4u	*C. neglecta*	0.00239	0.00045
Q1/B Tr11E Col H	MP114	4u	*C. neglecta*	0.00256	0.00045
Q1/B Tr11E Col H	MP114	4u	*C. neglecta*	0.00263	0.00042
Q1/B Tr11E Col H	MP114	4u	*C. neglecta*	0.00198	0.00034
Q1/B	202-105	4u	*C. neglecta*	0.00141	0.00062
Q1/B	202-105	4u	*C. neglecta*	0.00132	0.00039
Q1/B	202-105	4u	*C. neglecta*	0.00144	0.00038
Q1/B	202-105	4u	*C. neglecta*	0.00169	0.00038
Q1/B	202-105	4u	*C. neglecta*	0.00164	0.00035
				$\delta^{13}C$	$\delta^{18}O$
Q1/B Tr9	215/101	4u	*C. neglecta*	-7.68	-2.69
Q1/B Tr11E Col H	MP116	4u	*C. neglecta*	-7.86	-2.77
Q1/B Tr11E Col H	MP117	4u	*C. neglecta*	-7.71	-3.13
Q1/B Tr19-21	MP147	4u	*C. neglecta*	-7.61	-2.84
Q1/B Tr23E Col JK	MP156	3c	*C. neglecta*	-7.89	-2.54
Q1/B Tr23E Col JK	MP157	3c	*C. neglecta*	-7.40	-2.96
Q1/B Tr23E Col JK	MP158	4u	*C. neglecta*	-8.53	-2.40
Q1/B Tr17-18	MP160	4u(s)	*C. neglecta*	-7.74	-2.78
Q1/B Tr17-18	MP161	4u	*C. neglecta*	-8.67	-2.67
Q1/B Tr11E Col H	MP114	4u	*C. neglecta*	-7.94	-2.59
Q1/B	202-105	4u	*C. neglecta*	-7.96	-2.29
Q1/B D95 Tr9	215/101	4u	*P. zenkeri*	-7.69	-2.61
Q1/B Tr11E Col H	MP116	4u	*P. zenkeri*	-7.65	-3.01
Q1/B Tr11E Col H	MP117	4u	*P. zenkeri*	-7.09	-3.00
Q1/B Tr19-21	MP147	4u	*P. zenkeri*	-6.99	-2.79
Q1/B Tr23E Col JK	MP158	4u	*P. zenkeri*	-8.38	-2.93
Q1/B Tr17-18	MP160	4u(s)	*P. zenkeri*	-7.59	-2.72
Q1/B Tr17-18	MP161	4u	*P. zenkeri*	-7.83	-2.56
				$^{87}Sr/^{86}Sr$	
Q1/B Tr11E Col H	MP113	4u	*P. zenkeri*	0.70783	
Q1/B Tr11E Col H	MP113	4u	*C. neglecta*	0.70804	
Q1/B	MP 143	4u	*C. neglecta*	0.70791	
Q1/B	MP 143	4u	*P. zenkeri*	0.70778	
Q1/B Tr11E Col I	MP132	4u	*Ilyocypris monstrifica*	0.70782	
Q1/B Tr11E Col I	MP132	4u	*I. bradyi*	0.70777	
Q1/B Tr11E Col I	MP132	4u	*P. zenkeri*	0.70779	
Q1/B Tr11E Col H	MP115	4u	*C. neglecta*	0.70808	
Q1/B Tr11E Col H	MP115	4u	*P. zenkeri*	0.70810	
Q1/B Tr23E Col JK	MP158	4u	*C. neglecta*	0.70817	
Q1/B Tr23E Col JK	MP158	4u	*P. zenkeri*	0.70786	
Q1/B Tr23E Col JK	MP158	4u	*Elphidium williamsoni*	0.70907	
Q1/B Tr23E Col JK	MP158	4u	*Haynesina germanica*	0.70909	
Q1/B Tr23E Col JK	MP157	3c	*Elphidium williamsoni*	0.70912	
Q1/B Tr23E Col JK	MP157	3c	*Haynesina germanica*	0.70907	